

Parameter-Efficient Multi-Task Learning via Progressive Task-Specific Adaptation

Neeraj Gangwar^{†*} Anshuka Rangi[§] Rishabh Deshmukh[§] Holakou Rahamanian[§]
 Yesh Dattatreya[§] Nickvash Kani[†]
[†]University of Illinois Urbana-Champaign [§]Amazon

Abstract

Parameter-efficient fine-tuning methods have emerged as a promising solution for adapting pre-trained models to various downstream tasks. While these methods perform well in single-task learning, extending them to multi-task learning exacerbates common challenges, such as task interference and negative transfer, due to the limited number of trainable parameters. To address these issues, we introduce progressive task-specific multi-task adaptation, a novel parameter-efficient approach for multi-task learning. This approach introduces adapter modules in a pre-trained model such that these modules are shared across all tasks in the initial layers and become progressively more task-specific in the later layers. The motivation is to reduce the conflicts among tasks by allowing transfer learning across all tasks in the initial layers and enabling task-specific learning toward the prediction heads. Additionally, we propose a gradient-based approach for computing task similarity and use this measure to allocate similar tasks to the shared adapter modules. Our task similarity method introduces minimal overhead in the pipeline. We evaluate our approach by adapting the Swin Transformer for dense prediction tasks. Experiments on the PASCAL and NYUD-v2 datasets demonstrate that our approach outperforms a fully fine-tuned multi-task model while requiring only one-fifth of the trainable parameters. This approach achieves better relative improvement to single-task fine-tuning while reducing the number of trainable parameters and surpasses the current state-of-the-art methods for parameter-efficient multi-task learning.

1. Introduction

Large language and vision models pre-trained on extensive datasets have demonstrated an unprecedented ability to understand and generate human-like text and images, perform complex reasoning, and analyze data [1, 4, 14, 37, 38].

*Corresponding author (gangwar2@illinois.edu)

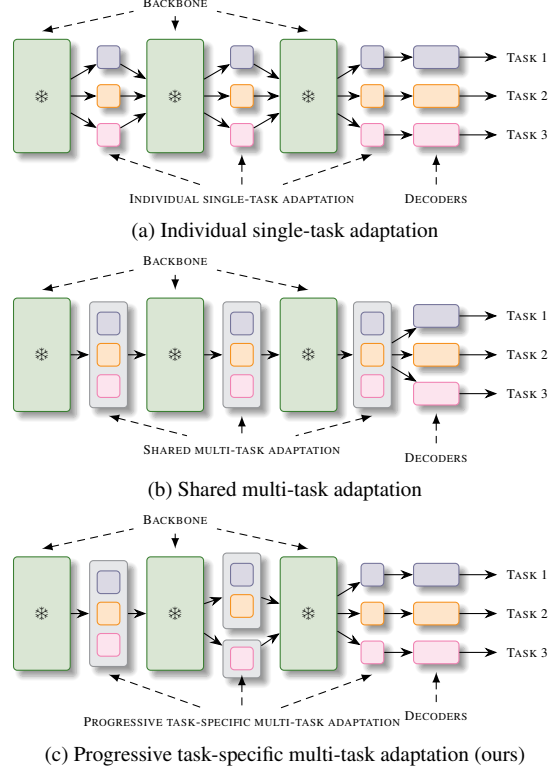


Figure 1. Approaches to adapt a pre-trained model to perform multiple tasks. (a) Individual single-task adaptation uses separate adapter modules for each task, resulting in no knowledge transfer, and the computational cost for inference grows with the number of tasks. (b) Shared adapter modules in shared multi-task adaptation result in lower inference cost but can suffer from task interference. (c) *Progressive task-specific multi-task adaptation*, where adapter modules become specific to a set of tasks toward the decoders, allowing knowledge transfer and task-specific learning.

These models can learn from a few demonstrations through in-context learning or can be adapted to various downstream tasks through targeted fine-tuning. Although fine-tuning may result in better performance compared to in-context learning, updating all model parameters demands substan-

tial computational resources. Additionally, separate copies of these models must be stored for each task that they are trained to handle. These challenges are further intensified as the model sizes continue to grow.

Several parameter-efficient methods have been proposed to address these challenges [17, 18, 22, 23, 25, 36, 50]. These approaches either fine-tune a subset of the model’s existing parameters or add new layers, training only these layers. In both cases, the number of trainable parameters remains small relative to the overall model size. These methods have achieved performance levels that nearly match those of full fine-tuning, offering a more favorable trade-off between trainable parameter count and downstream task performance. They also reduce the storage requirements, as only the updated parameters must be stored separately for each task. These methods have been widely used for adapting large language models to various natural language processing (NLP) and vision tasks [7, 10, 19, 20, 44]. While they have proven highly effective for adapting single-task models, their applicability to multi-task learning (MTL) remains limited. One reason is the unique challenges associated with MTL. Due to the sharing of parameters across tasks, MTL can suffer from conflicting and dominating gradients. This results in interference and negative transfer between tasks, leading to significantly degraded performance [48]. These problems become more pronounced in parameter-efficient multi-task learning (PEMTL), as the limited number of trainable parameters restricts the model’s capacity to effectively separate task-specific knowledge. Although PEMTL is relatively underexplored, several works have recently made notable advancements [3, 26, 30, 33, 43].

Existing methods for adapting a pre-trained model to perform multiple tasks fall into two main categories – (1) individual single-task adaptation and (2) shared multi-task adaptation. In individual single-task adaptation (Figure 1a), separate adapter modules¹ are added for each downstream task, making it particularly effective when tasks are not related or have specific requirements. However, there are two major drawbacks. First, this method does not allow for knowledge transfer among tasks, which may lead to suboptimal performance compared to models with shared parameters. Second, the computational cost of inference increases linearly with the number of tasks, as the adapter modules for each task must be executed individually. In shared multi-task adaptation (Figure 1b), the adapter modules are shared across all tasks. This setup enables knowledge transfer between tasks and offers improved inference cost over individual single-task adaptation. However, due to gradient conflicts, shared adapter modules can suffer from task interference and negative transfer, limiting task-specific learning.

¹We use the term “adapter module” to refer to the parameters added to a model to adapt it for a downstream task.

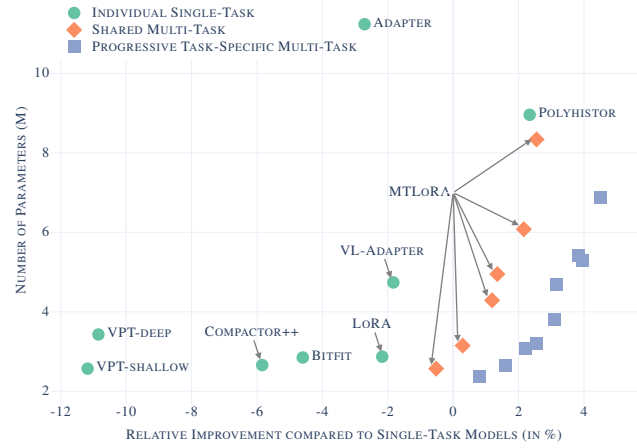


Figure 2. Comparison of our proposed approach, progressive task-specific multi-task adaptation, with methods that use individual single-task and shared multi-task adaptations. These experiments are performed on the PASCAL dataset with the Swin-Tiny version of the Swin Transformer. The numbers for individual single-task and shared multi-task adaptations are taken from Agiza et al. [3].

To address these issues, we introduce *progressive task-specific multi-task adaptation*, a parameter-efficient approach illustrated in Figure 1c. Our approach sits between the two extremes of individual single-task and shared multi-task adaptations. In our approach, the adapter modules are shared among all tasks in the early layers, and they become increasingly specific to a subset of tasks as we move toward task-specific decoders. Structuring adapter modules in this manner effectively forms a branched multi-task network. While branched networks have been effective in full fine-tuning settings [6, 15, 29, 39], the branching significantly increases trainable parameters and storage requirements. Adapter modules offer a more efficient way of implementing branching while maintaining strong multi-task performance with substantially fewer trainable parameters. Our approach achieves inference cost that falls between those of individual single-task and shared multi-task adaptations. To reduce conflicts among tasks, we assign *similar* tasks to the shared adapter modules. We use a gradient-based method to compute task similarity, which introduces minimal computational overhead. We hypothesize that a progressive task-specific architecture could better handle task conflicts and improve performance with fewer trainable parameters. We compare our approach with the existing PEMTL methods on the PASCAL and NYUD-v2 datasets.

Contributions. We summarize the contributions of our work below:

1. We introduce progressive task-specific adaptation, a parameter-efficient method for multi-task learning that sits between individual single-task and shared multi-task

adaptations. It allows for knowledge transfer among tasks while reducing task interference through intelligent grouping.

2. We propose a gradient-based task similarity approach that is used to assign similar tasks to the shared adapter modules. Our experiments show that grouping less similar tasks, identified by this approach, adversely impacts the multi-task model’s performance, proving its effectiveness.
3. We create a LoRA-based [18] layer named TGLoRA, which is used to implement the progressive task-specific architecture.
4. Our approach achieves better relative improvement to the single-task fine-tuning while using fewer trainable parameters than the current state-of-the-art PEMTL approaches. Figure 2 shows a comparison of our approach with the existing approaches on the PASCAL dataset.

2. Related Works

Parameter-Efficient Fine-Tuning. To achieve a better trade-off between the number of trainable parameters and performance on the downstream tasks, various methods have been proposed. These approaches fine-tune a small set of parameters while the rest of the model is frozen. One set of approaches adds new layers to the model and fine-tunes only these. For example, Houlsby et al. [17] and Pfeiffer et al. [32] placed Adapter layers after the attention and MLP layers and fine-tuned these newly added layers to achieve a comparable performance to full fine-tuning on NLP datasets. Hu et al. [18] proposed LoRA, a method to efficiently fine-tune large language models by adding low-rank decomposition matrices to their weights, significantly reducing the number of trainable parameters. Several subsequent works have proposed variations of LoRA, for example, AdaLoRA [50], LoRA Dropout [24], DoRA [25], and LoRA+ [16], among others. Another line of research adds trainable prompts to the input and fine-tunes only these while keeping the model frozen [22, 23]. Methods like BitFit [49] and FISH [36] fine-tune a small set of the model’s parameters without adding any new parameters to the model. While parameter-efficient methods have been majorly applied to NLP tasks, several works have explored their application for vision tasks. Jia et al. [20] proposed visual prompt tuning for adapting Vision Transformers. Gao et al. [14] proposed Llama-Adapter V2, which leverages both prefix-tuning and adapter techniques.

Multi-Task Learning. MTL in computer vision aims to train a model to perform multiple related tasks simultaneously, such as object detection, segmentation, depth estimation, etc. By sharing representations across tasks, MTL allows models to leverage shared information, potentially improving performance and efficiency compared to training

separate models for each task [11, 41, 47]. However, MTL faces some common challenges, such as task interference, negative transfer, and task dominance. Several methods have been proposed to mitigate these issues in a full fine-tuning setting [5, 9, 21, 31, 34]. Another line of research has focused on branched multi-task networks [6, 15, 29, 39]. The branching aims to balance shared representations and task-specific learning for improved performance and efficiency. While some works use neural architecture search [6] or reinforcement learning [15], our approach aligns with methods that leverage task affinity to group similar tasks [13, 39]. However, unlike these methods, our approach does not rely on training separate models to compute task similarity, making it more efficient. Other methods to compute task similarity have also used Fisher information [2]. Instead, we compute similarity directly from gradients.

Parameter-Efficient Multi-Task Learning. PEMTL is relatively under-explored; however, there are some notable contributions. To address the lack of knowledge transfer in individual single-task adaptation, Mahabadi et al. [30] proposed Hyperformer, which uses a common hypernetwork to generate Adapter module parameters for different tasks, fine-tuning only the hypernetwork. This approach facilitates knowledge transfer across tasks via the shared hypernetwork. Liu et al. [26] proposed Polyhisto, a more parameter-efficient version of Hyperformer for dense vision tasks. While this approach enables knowledge transfer, the inference cost still increases linearly with the number of tasks. To address this, Agiza et al. [3] introduced MTLoRA, closely approximating shared multi-task adaptation. Unlike shared multi-task adaptation, which relies solely on shared modules, MTLoRA incorporates task-specific modules in certain layers to enable task-specific learning. Although this mitigates some interference, most layers in MTLoRA remain shared across tasks, leading to task conflicts. Additionally, the number of task-specific modules scales linearly with the task count.

3. Proposed Approach

We hypothesize that leveraging task similarity can enhance knowledge transfer across tasks while reducing conflicts, boosting multi-task performance with fewer trainable parameters. Based on this, we introduce *progressive task-specific multi-task adaptation* of pre-trained models, which balances the two extremes of individual single-task and shared multi-task adaptations. In our approach, adapter modules are shared among tasks in early layers and gradually become more task-specific in later layers. To reduce task interference, we assign similar tasks to an adapter module. This intelligent parameter sharing allows for effective knowledge transfer among tasks while reducing task conflicts, addressing both the knowledge transfer limitations of

individual single-task adaptation and the task interference challenges of shared multi-task adaptation. This architecture achieves better inference cost than individual single-task adaptation by significantly reducing the number of dedicated adapter modules. With moderately higher inference cost than shared multi-task adaptation, this architecture offers significant performance improvement.

We define a *task group* as a set of tasks assigned to a single adapter module. Adding multiple adapter modules for different task groups within a layer effectively creates copies of that layer, with each copy specialized for a particular task group. Each copy's parameters are updated based on the combined loss for its respective task group. As a result, the progressive task-specific adaptation shown in Figure 1c is equivalent to transforming a linear architecture to a tree-like structure, where task-specific decoders serve as leaves. Each path from the root to a leaf represents a different task, and a task's path can be identified by the specific decoder at its endpoint. The tree-like structure ensures the task specificity of adapter modules. While this architecture could demand significant memory and training cost with full fine-tuning, it can be efficiently implemented with adapter modules. Notably, adapter modules in the final layer can be shared across multiple tasks rather than being task-specific. This helps to limit the proliferation of adapter modules and manage the resulting tree's width in the case of extreme MTL, addressing the linear expansion of task-specific modules observed in MTLoRA.

The number of task groups in a layer is decided based on the following constraints to maintain the task specificity of adapter modules

- Every layer has the same or more task groups than the previous layers.
- Two tasks in a task group of a layer do not belong to different task groups in any of the previous layers.

This means a task group can only be split into multiple in the subsequent layers but never merged.

3.1. Task Similarity

We use the notion of gradient conflicts from the MTL literature to compute the similarity between a pair of tasks. Formally, consider a set of tasks $\mathcal{T} = \{1, 2, \dots, T\}$ and model parameters $\{\theta_s\} \cup \{\theta_t | t \in \mathcal{T}\}$, where θ_s and θ_t represent the shared and task-specific parameters, respectively. Let $\mathcal{D}_t = \{x_{t,i} | 1 \leq i \leq |\mathcal{D}_t|\}$ represent the training dataset for task t . We define the similarity between two tasks based on the gradient of each task's loss with respect to the shared parameters. Specifically, the similarity between tasks t and t' is given by

$$\mathbb{E}_{x \sim \mathcal{D}_t, x' \sim \mathcal{D}_{t'}} [S(g(x, t), g(x', t'))] \quad (1)$$

$$g(x, t) = \nabla_{\theta_s} \mathcal{L}(\theta_s, \theta_t, x)$$

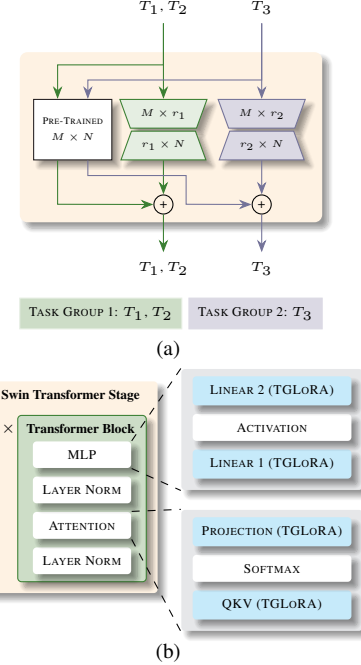


Figure 3. (a) TGLoRA Layer with two task groups. T_1, T_2 , and T_3 represent three tasks. (b) TGLoRA is added to the attention and MLP layers of the Swin Transformer.

where S and $\mathcal{L}(\cdot)$ represent the similarity and loss functions. Following Achille et al. [2], we use the cosine similarity, indicated by S_{\cos} , between the normalized gradients to compute the similarity as follows

$$S(g, g') = S_{\cos} \left(\frac{g}{\|g\| + \|g'\|}, \frac{g'}{\|g\| + \|g'\|} \right) \quad (2)$$

Here, g and g' are shorthands for $g(x, t)$ and $g(x', t')$, respectively. Note that (1) does not constrain that the inputs must be the same for all tasks and may be applied to tasks not sharing the same inputs.

We use a pre-trained backbone (θ_s) with task-specific heads (θ_t 's) to compute the similarity. The task-specific heads are randomly initialized, so we fine-tuned them on the training examples. The backbone remains frozen during this fine-tuning. For our experiments, the expectation, \mathbb{E} , in (1) is replaced by the empirical mean, and the similarity is computed as

$$\frac{1}{N} \sum_{i=1}^N S(g(x_{t,i}, t), g(x'_{t,i}, t')) \quad (3)$$

where N represents the number of examples used for similarity computation. As our task similarity is defined as the expectation of example-level similarity, we ensure that no model parameters are disabled in the forward pass due to the dropout layer.

3.2. Task-Grouped LoRA (TGLoRA)

To implement the progressive task-specific architecture, we create a LoRA-based layer [18] – *Task-Grouped LoRA* or *TGLoRA*. It consists of multiple low-rank modules, one for each task group. It takes as many inputs as the number of task groups and produces those many outputs. Let $W \in \mathbb{R}^{d \times k}$ represent a pre-trained weight matrix and $A_\pi \in \mathbb{R}^{r_\pi \times k}$ and $B_\pi \in \mathbb{R}^{d \times r_\pi}$ represent low-rank matrices with rank r_π for task group π . The input corresponding to task group π , $x_\pi \in \mathbb{R}^k$, is processed as

$$y_\pi = W x_\pi + \gamma_{r,\pi} B_\pi A_\pi x_\pi \quad (4)$$

where $\gamma_{r,\pi} = \frac{\alpha_\pi}{r_\pi}$ represents the scaling factor defined in Hu et al. [18]. Figure 3a shows this layer for two task groups. Note that a TGLoRA layer with one task group reduces to a LoRA layer. Figure 3b illustrates the augmentation of the Swin Transformer with these layers.

3.3. Computing Task Groups

Creating task groups is a set partitioning problem. Formally, it can be defined as partitioning \mathcal{T} into a partition $P = \{\pi_1 \dots \pi_M\}$ such that

- $\bigcup_{i=1}^M \pi_i = \mathcal{T}$; and
- $\pi_i \cap \pi_j = \emptyset \forall 1 \leq i, j \leq M$ and $i \neq j$

We assign a score to every partition P , based on the tasks in each group π_i , which we define momentarily. Intuitively, this score should be higher when similar tasks are grouped and lower when conflicting tasks are assigned to the same task group. This score is determined by evaluating the affinity of each task with other tasks within its respective group. Our objective is to find a partition with the highest score.

First, we assign a score to each task t in a task group π_i as

$$\mathcal{S}_{t,\pi_i} = \begin{cases} 0 & |\pi_i| = 1 \\ \frac{\sum_{t' \in \pi_i, t' \neq t} \text{sim}(t, t')}{|\pi_i| - 1} & \text{Otherwise} \end{cases} \quad (5)$$

where $\text{sim}(t, t')$ is the task similarity defined in (3). The score for partition P is defined as

$$\mathcal{S}_P = \sum_{i=1}^M \sum_{t \in \pi_i} \mathcal{S}_{t,\pi_i} \quad (6)$$

To convert a pre-trained model to a branched network, task groups are computed in reverse. We first compute the task groups for the layer just before the decoders. If this layer has task-specific modules with no sharing, we partition \mathcal{T} into subsets of size one and move on to the layer preceding it. The branch-and-bound algorithm [13] is used to find the partition that maximizes \mathcal{S}_P . For every other layer, we either keep the same task groups as the next layer or merge the task groups to achieve the required number of groups. Algorithm 1 is used to merge the task groups.

Algorithm 1 Task Group Merging.

Require: Tasks $\mathcal{T} = \{1 \dots T\}$, a set of task groups $P = \{\pi_1 \dots \pi_M\}$, task similarities $\{\mathcal{S}_{t,t'} | t, t' \in \mathcal{T}\}$, $N < M$

1: $Q \leftarrow P$ ▷ Partition after merging

2: **repeat**

3: $Q' \leftarrow \emptyset$ ▷ Best partition after merging two groups

4: $s \leftarrow 0$ ▷ Score for the best partition

5: **for all** $\pi_i, \pi_j \in Q$ **do**

6: $P' \leftarrow (P \setminus \{\pi_i, \pi_j\}) \cup \{\pi_i \cup \pi_j\}$ ▷ Defined in (6)

7: $s' \leftarrow \mathcal{S}_{P'}$ ▷ Defined in (6)

8: **if** $s' > s$ **then**

9: $s \leftarrow s'$

10: $Q' \leftarrow P'$

11: **end if**

12: **end for**

13: $Q \leftarrow Q'$

14: **until** $|Q| = N$

15: **return** Q

4. Experiments

4.1. Dataset

Following previous works in the MTL literature [3, 26, 40, 45, 46], we evaluate our approach on the PASCAL [12] and NYUD-v2 [35] datasets. We use the PASCAL-Context split [8] for PASCAL. It has four dense prediction tasks – (1) semantic segmentation, (2) saliency detection, (3) surface normal estimation, and (4) human part segmentation. The dataset consists of training and validation splits with 4,998 and 5,105 images, respectively. We consider three tasks in the NYUD-v2 dataset – (1) semantic segmentation, (2) depth estimation, and (3) surface normal estimation. The dataset contains 795 training and 654 validation examples.

4.2. Evaluation Metrics

The performance on semantic segmentation, saliency detection, and human part segmentation is evaluated using mean intersection-over-union (mIoU). Surface normal estimation and depth estimation are evaluated using root mean square error (rmse). Following previous works on MTL [3, 26, 41], we use the number of trainable parameters and the average per-task difference in performance compared to single-task full fine-tuning (Δm) to evaluate multi-task models. Δm is defined as

$$\Delta m = \frac{1}{T} \sum_{t=1}^T (-1)^{l_t} \frac{M_t - M_{st,t}}{M_{st,t}} \quad (7)$$

where M_t and $M_{st,t}$ represent the multi-task and single-task models’ performances on task t , respectively. l_t is 0 if a higher score means better performance for task t and is 1 otherwise.

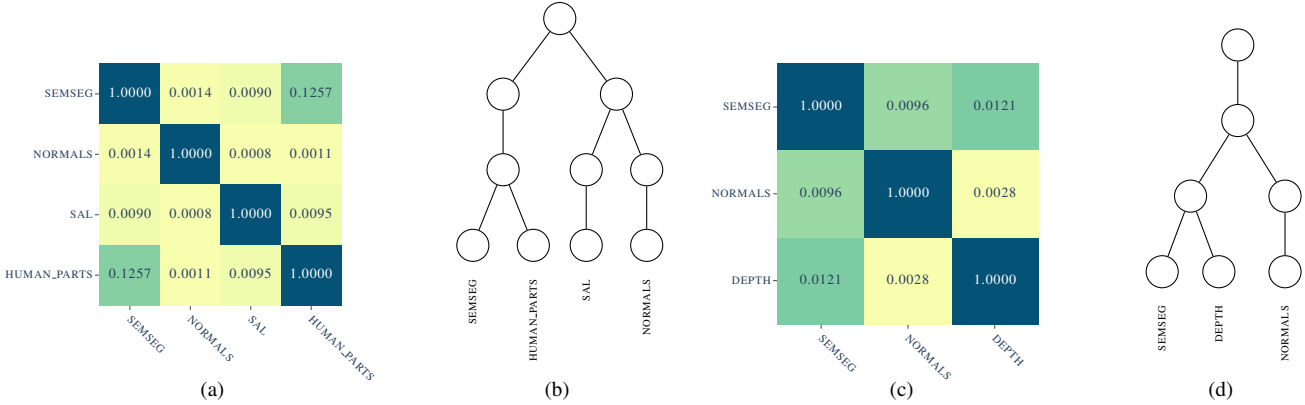


Figure 4. (a) and (b) illustrate the task similarities and computed task groups for PASCAL, respectively, while (c) and (d) present the same information for NYUD-v2. The four levels in the trees represent the four stages of the Swin Transformer.

4.3. Setup

Base Model. We replicate the model architecture from Agiza et al. [3] for a fair comparison with the existing methods. Specifically, we use the Swin Transformer [27] and attach task-specific decoders for each task. The task-specific decoders are similar to the one used in HR-Net [42], consisting of linear and bilinear upsampling layers. For the Swin Transformer, we use the Swin-Tiny variant pre-trained on ImageNet-1k. Furthermore, we use multi-scale task-specific feature sharing in MTLoRA, which merges features from different stages for a comprehensive feature representation. See Agiza et al. [3] for more details on multi-scale task-specific feature sharing.

Optimization. The models are trained to minimize the multi-task loss

$$L_{\text{MTL}} = \sum_{t=1}^T w_t \times L_t \quad (8)$$

where w_t and L_t are the task weight and loss for task t . Task weights are the same as in previous works [3, 26]. We use per-pixel cross-entropy loss for semantic segmentation and human part segmentation, L1 loss for surface normal and depth estimations, and balanced cross-entropy loss for saliency detection.

Trainable Layers. We conduct our experiments by adding TGLoRA modules to the attention (indicated by “ATTN”) and MLP (indicated by “MLP”) layers (Figure 3b). We determine the rank of the low-rank matrices for each task group in a TGLoRA layer based on the number of tasks in the task group. Using a combined rank r for a TGLoRA layer, we allocate it proportionally across different task groups. This strategy ensures better control of the trainable parameter count across different configurations. In

the case of the PASCAL dataset, where the final stage consists of four task groups with one task each, we assign a fixed rank of four to each low-rank matrix. Although we keep the rank constant in the last stage regardless of the value of r , it could also be scaled according to r , which would simply increase the number of trainable parameters. Additionally, similar to MTLoRA, we explore unfreezing the patch embedding, patch merging, layer normalization, and position bias layers (indicated by “OTHERS”).

Training Details. We repeat each experiment three times with different random seeds and report the average scores. See Section 7 in the supplementary material for the hyperparameters used for training.

4.4. Task Group Creation

We determine the number of task groups in each TGLoRA layer according to a predefined computational budget, such as parameter count or floating-point operations per second (FLOPS). For simplicity, we do not change the number of task groups in the TGLoRA layers within a stage of the Swin Transformer. We keep the first stage shared, the last stage task-specific, and reduce the number of task groups by one as we move away from the decoders. Figure 4 shows the task similarities and task groups computed by our method for the PASCAL and NYUD-v2 datasets. The influence of varying computational budgets is discussed in Section 9 of the supplementary material.

We use the Swin Transformer with task-specific decoders to compute the task similarity. As discussed in Section 3.1, fine-tuning the decoders is necessary for computing task similarity. We examine the impact of fine-tuning with a limited subset of training examples versus the full training dataset. Our experiments show that both approaches produce identical task groups. Furthermore, repeating the fine-tuning process three times with different

Table 1. Comparison of progressive task-specific adaptation (indicated by TGLoRA) with the existing methods on PASCAL-Context. \uparrow and \downarrow signify that higher and lower values are better, respectively. Results marked with \dagger are from Agiza et al. [3]. The experiments are repeated three times with different random seeds, and the averages are reported.

Method	SemSeg (mIoU \uparrow)	Human Parts (mIoU \uparrow)	Saliency (mIoU \uparrow)	Normals (rmse \downarrow)	Δm (% \uparrow)	Trainable Params (M \downarrow)
Single Task – Full Fine-Tuning \dagger	67.21	61.93	62.35	17.97	0	112.62
MTL – Decoders Only \dagger	65.09	53.48	57.46	20.69	-9.95	1.94
MTL – Full Fine-Tuning \dagger	67.56	60.24	65.21	16.64	+2.23	30.06
Hyperformer \dagger [26, 30]	71.43	60.73	65.54	17.77	+2.64	72.77
Polyhisto \dagger [26]	70.87	59.15	65.54	17.77	+2.34	8.96
MTLoRA \dagger [3]	67.90	59.84	65.40	16.60	+2.55	8.34
MTL – LoRA [18] (ATTN + MLP)	67.57	59.09	65.18	17.08	+1.36	5.29
Single Task – LoRA [18] (ATTN + MLP)	70.80	58.73	66.05	16.65	+3.36	5.29
TGLoRA (ATTN + MLP + OTHERS)	70.53	60.96	66.12	16.43	+4.50	6.89
TGLoRA (ATTN + MLP)	70.39	60.58	65.94	16.61	+3.97	5.29
TGLoRA (ATTN)	70.27	59.36	65.38	17.09	+2.54	3.20

random seeds confirms the consistency of the results. These results suggest that this fine-tuning step introduces minimal overhead in the training pipeline.

4.5. Results

We compare our approach against existing PEMTL methods – Polyhisto [26] and MTLoRA [3] – on PASCAL and against MTLoRA [3] on NYUD-v2. Additionally, we include two baseline methods:

- *Single Task – LoRA*: We fine-tune single-task models by adding LoRA modules to the attention and MLP layers. As there are no shared parameters, this setting does not allow for knowledge transfer among tasks.
- *MTL – LoRA*: We also fine-tune a multi-task model by adding LoRA modules to the attention and MLP layers. This baseline represents another extreme where all trainable parameters, except for the decoders, are shared.

For both baselines, we ensure that the total number of parameters across tasks is the same as that in the corresponding progressive task-specific multi-task model that uses TGLoRA.

MTL Performance. Tables 1 and 2 show the per-task performance, the overall MTL performance (Δm), and the number of trainable parameters for PASCAL and NYUD-v2, respectively. The results indicated by \dagger are taken from Agiza et al. [3]. For PASCAL, our approach achieves more than 2% absolute improvement in the overall MTL performance over MTLoRA and Polyhisto while using significantly fewer trainable parameters (indicated by ATTN + MLP + OTHERS). Furthermore, it surpasses Hyperformer by a significant margin, which requires considerably more trainable parameters. Similar to Agiza et al. [3], we also observe improved performance by unfreezing additional lay-

ers compared to only fine-tuning the newly added TGLoRA modules (indicated by ATTN + MLP). As a final point, adding TGLoRA only to the attention layers is very effective and achieves comparable performance to MTLoRA and Polyhisto while requiring less than half the trainable parameters (indicated by ATTN). For NYUD-v2, our approach outperforms MTLoRA by more than 1% while using fewer trainable parameters. Moreover, it achieves better overall MTL performance than MTLoRA while keeping additional layers frozen during fine-tuning, leading to a significantly better trade-off between the number of trainable parameters and performance.

For both datasets, the progressive task-specific architecture performs better than the single-task (indicated by “Single Task – LoRA”) and multi-task models (indicated by “MTL – LoRA”) with a shared backbone for the same parameter budget. This behavior remains consistent when adding TGLoRA only to the attention layer and unfreezing additional layers during training. Note that unfreezing additional layers results in more trainable parameters in the single-task models, as these layers must be unfrozen in individual models. See Section 8 in the supplementary material for additional results.

Inference Cost. Table 3 shows the number of giga multiply-accumulate operations for our approach compared to individual single-task and shared multi-task adaptations. These results show that the inference cost for progressive task-specific adaptations lies between the two extremes.

4.6. Sub-Optimal Task Groups

Next, we examine the impact of grouping less similar tasks, as per the task similarities shown in Figure 4, while keeping the number of task groups unchanged. For PASCAL,

Table 2. Comparison of progressive task-specific adaptation (indicated by TGLoRA) with the existing methods on NYUD-v2. \uparrow and \downarrow signify that higher and lower values are better, respectively. The experiments are repeated three times with different random seeds, and the averages are reported.

Method	SemSeg (mIoU \uparrow)	Normals (rmse \downarrow)	Depth (rmse \downarrow)	Δm (% \uparrow)	Trainable Params (M \downarrow)
Single Task – Full Fine-Tuning	41.85	24.01	0.6322	0	83.99
MTL – Full Fine-Tuning	41.17	24.75	0.6217	-1.01	29.00
MTL – Decoder Only	35.97	32.63	0.8008	-25.54	1.48
MTLoRA [3]	41.52	24.99	0.6212	-1.04	7.81
MTL – LoRA [18] (ATTN + MLP)	41.05	25.01	0.6231	-1.54	5.93
Single Task – LoRA [18] (ATTN + MLP)	41.86	24.57	0.6295	-0.63	5.93
TGLoRA (ATTN + MLP + OTHERS)	41.84	24.38	0.6177	+0.24	7.53
TGLoRA (ATTN + MLP)	41.89	24.45	0.6236	-0.12	5.93
TGLoRA (ATTN)	41.92	25.27	0.6319	-1.68	3.15

Table 3. Giga multiply-accumulate operations for individual single-task, shared multi-task, and progressive task-specific multi-task adaptations.

Dataset	#Tasks	Individual Single-Task	Shared Multi-Task	Progressive Task-Specific
PASCAL	1	18.49	18.49	18.49
	4	73.96	21.47	49.95
NYUD-v2	1	18.56	18.56	18.56
	3	55.41	20.53	34.65

we swap saliency and human part segmentation in the second and third stages of the Swin Transformer. Similarly, we swap depth and surface normal estimation tasks in the third stage for NYUD-v2. The MTL performance under these configurations is illustrated in Table 4. These results demonstrate that grouping less similar tasks adversely impacts the model’s performance, providing strong evidence in favor of our proposed method of computing task similarity and forming task groups.

5. Conclusion

In this work, we introduced progressive task-specific multi-task adaptation, positioned between individual single-task and shared multi-task adaptations. To implement it, we developed a new LoRA-based layer named TGLoRA and a gradient-based metric to measure task similarity. We adapted the Swin Transformer for dense prediction tasks and evaluated our approach using the PASCAL and NYUD-v2 multi-task datasets. Our experimental results showed that progressive task-specific adaptation outperforms both individual single-task and shared multi-task adaptations, achieving significantly greater relative improvement over single-task models while using fewer trainable parameters than the current state-of-the-art approaches. Ablation stud-

Table 4. Performance of progressive task-specific adaptation with TGLoRA when less similar tasks are in the same task group. Δm is computed based on the single-task performance from Table 1 for PASCAL and Table 2 for NYUD-v2. The experiments are repeated three times with different random seeds, and the averages are reported.

Dataset	Method	Δm (% \uparrow)	Trainable Params (M \downarrow)
PASCAL	ATTN + MLP + OTHERS	+3.71	6.89
	ATTN + MLP	+3.14	5.29
	ATTN	+1.95	3.20
NYUD-v2	ATTN + MLP + OTHERS	-1.11	7.53
	ATTN + MLP	-0.90	5.93
	ATTN	-2.30	3.15

ies demonstrated that grouping less similar tasks adversely affects multi-task performance, highlighting the effectiveness of our method. Experiments also showed that our task similarity method introduces minimal overhead in the training pipeline.

6. Limitations

In our experiments, we progressively increase the number of task groups across stages in a predefined manner. Exploring different configurations could provide valuable insights and improve our approach’s effectiveness. Moreover, an automated method to compute the optimal number of task groups would be beneficial. Another limitation of our work is related to the task grouping algorithm. We use a branch-and-bound-like algorithm to compute task groups in the last stage, which is manageable for a small set of tasks but quickly becomes impractical as the number of tasks grows. An approximate version of this algorithm could help scale our approach to extreme MTL settings. We leave these avenues for future research.

References

[1] Josh Achiam, Steven Adler, Sandhini Agarwal, Lama Ahmad, Ilge Akkaya, Florencia Leoni Aleman, Diogo Almeida, Janko Altenschmidt, Sam Altman, Shyamal Anadkat, et al. Gpt-4 technical report. *arXiv preprint arXiv:2303.08774*, 2023. 1

[2] Alessandro Achille, Michael Lam, Rahul Tewari, Avinash Ravichandran, Subhransu Maji, Charless C Fowlkes, Stefano Soatto, and Pietro Perona. Task2vec: Task embedding for meta-learning. In *Proceedings of the IEEE/CVF international conference on computer vision*, pages 6430–6439, 2019. 3, 4

[3] Ahmed Agiza, Marina Neseem, and Sherief Reda. MT-LoRA: Low-rank adaptation approach for efficient multi-task learning. In *Proceedings of the IEEE/CVF Conference on Computer Vision and Pattern Recognition*, pages 16196–16205, 2024. 2, 3, 5, 6, 7, 8, 1

[4] Yutong Bai, Xinyang Geng, Karttikeya Mangalam, Amir Bar, Alan L Yuille, Trevor Darrell, Jitendra Malik, and Alexei A Efros. Sequential modeling enables scalable learning for large vision models. In *Proceedings of the IEEE/CVF Conference on Computer Vision and Pattern Recognition*, pages 22861–22872, 2024. 1

[5] Hao Ban and Kaiyi Ji. Fair resource allocation in multi-task learning. In *Forty-first International Conference on Machine Learning*, 2024. 3

[6] David Brüggemann, Menelaos Kanakis, Stamatios Georgoulis, and Luc Van Gool. Automated search for resource-efficient branched multi-task networks. In *31st British Machine Vision Conference 2020, BMVC 2020*, page 359. BMVA Press, 2020. 2, 3

[7] Shoufa Chen, Chongjian Ge, Zhan Tong, Jiangliu Wang, Yibing Song, Jue Wang, and Ping Luo. Adaptformer: Adapting vision transformers for scalable visual recognition. *Advances in Neural Information Processing Systems*, 35:16664–16678, 2022. 2

[8] Xianjie Chen, Roozbeh Mottaghi, Xiaobai Liu, Sanja Fidler, Raquel Urtasun, and Alan Yuille. Detect what you can: Detecting and representing objects using holistic models and body parts. In *Proceedings of the IEEE conference on computer vision and pattern recognition*, pages 1971–1978, 2014. 5

[9] Zhao Chen, Vijay Badrinarayanan, Chen-Yu Lee, and Andrew Rabinovich. Gradnorm: Gradient normalization for adaptive loss balancing in deep multitask networks. In *International conference on machine learning*, pages 794–803. PMLR, 2018. 3

[10] Zhe Chen, Yuchen Duan, Wenhui Wang, Junjun He, Tong Lu, Jifeng Dai, and Yu Qiao. Vision transformer adapter for dense predictions. In *The Eleventh International Conference on Learning Representations*, 2023. 2

[11] Michael Crawshaw. Multi-task learning with deep neural networks: A survey. *arXiv preprint arXiv:2009.09796*, 2020. 3

[12] Mark Everingham, Luc Van Gool, Christopher KI Williams, John Winn, and Andrew Zisserman. The pascal visual object classes (voc) challenge. *International Journal of Computer Vision*, 88:303–338, 2010. 5

[13] Chris Fifty, Ehsan Amid, Zhe Zhao, Tianhe Yu, Rohan Anil, and Chelsea Finn. Efficiently identifying task groupings for multi-task learning. *Advances in Neural Information Processing Systems*, 34:27503–27516, 2021. 3, 5

[14] Peng Gao, Jiaming Han, Renrui Zhang, Ziyi Lin, Shijie Geng, Aojun Zhou, Wei Zhang, Pan Lu, Conghui He, Xiangyu Yue, et al. Llama-adapter v2: Parameter-efficient visual instruction model. *arXiv preprint arXiv:2304.15010*, 2023. 1, 3

[15] Pengsheng Guo, Chen-Yu Lee, and Daniel Ulbricht. Learning to branch for multi-task learning. In *International conference on machine learning*, pages 3854–3863. PMLR, 2020. 2, 3

[16] Soufiane Hayou, Nikhil Ghosh, and Bin Yu. Lora+: Efficient low rank adaptation of large models. In *Forty-first International Conference on Machine Learning*, 2024. 3

[17] Neil Houlsby, Andrei Giurgiu, Stanislaw Jastrzebski, Bruna Morrone, Quentin De Laroussilhe, Andrea Gesmundo, Mona Attariyan, and Sylvain Gelly. Parameter-efficient transfer learning for nlp. In *International conference on machine learning*, pages 2790–2799. PMLR, 2019. 2, 3

[18] Edward J Hu, Phillip Wallis, Zeyuan Allen-Zhu, Yuanzhi Li, Shean Wang, Lu Wang, Weizhu Chen, et al. LoRA: Low-rank adaptation of large language models. In *International Conference on Learning Representations*, 2022. 2, 3, 5, 7, 8

[19] Zhiqiang Hu, Lei Wang, Yihuai Lan, Wanyu Xu, Ee-Peng Lim, Lidong Bing, Xing Xu, Soujanya Poria, and Roy Lee. Llm-adapters: An adapter family for parameter-efficient fine-tuning of large language models. In *Proceedings of the 2023 Conference on Empirical Methods in Natural Language Processing*, pages 5254–5276, 2023. 2

[20] Menglin Jia, Luming Tang, Bor-Chun Chen, Claire Cardie, Serge Belongie, Bharath Hariharan, and Ser-Nam Lim. Visual prompt tuning. In *European Conference on Computer Vision*, pages 709–727. Springer, 2022. 2, 3

[21] Alex Kendall, Yarin Gal, and Roberto Cipolla. Multi-task learning using uncertainty to weigh losses for scene geometry and semantics. In *Proceedings of the IEEE conference on computer vision and pattern recognition*, pages 7482–7491, 2018. 3

[22] Brian Lester, Rami Al-Rfou, and Noah Constant. The power of scale for parameter-efficient prompt tuning. In *Proceedings of the 2021 Conference on Empirical Methods in Natural Language Processing*, pages 3045–3059, 2021. 2, 3

[23] Xiang Lisa Li and Percy Liang. Prefix-tuning: Optimizing continuous prompts for generation. In *Proceedings of the 59th Annual Meeting of the Association for Computational Linguistics and the 11th International Joint Conference on Natural Language Processing (Volume 1: Long Papers)*, pages 4582–4597, 2021. 2, 3

[24] Yang Lin, Xinyu Ma, Xu Chu, Yujie Jin, Zhibang Yang, Yasha Wang, and Hong Mei. Lora dropout as a sparsity regularizer for overfitting control. *arXiv preprint arXiv:2404.09610*, 2024. 3

[25] Shih-yang Liu, Chien-Yi Wang, Hongxu Yin, Pavlo Molchanov, Yu-Chiang Frank Wang, Kwang-Ting Cheng,

and Min-Hung Chen. Dora: Weight-decomposed low-rank adaptation. In *Forty-first International Conference on Machine Learning*, 2024. 2, 3

[26] Yen-Cheng Liu, Chih-Yao Ma, Junjiao Tian, Zijian He, and Zsolt Kira. Polyhistor: Parameter-efficient multi-task adaptation for dense vision tasks. *Advances in Neural Information Processing Systems*, 35:36889–36901, 2022. 2, 3, 5, 6, 7

[27] Ze Liu, Yutong Lin, Yue Cao, Han Hu, Yixuan Wei, Zheng Zhang, Stephen Lin, and Baining Guo. Swin transformer: Hierarchical vision transformer using shifted windows. In *Proceedings of the IEEE/CVF International Conference on Computer Vision*, pages 10012–10022, 2021. 6

[28] Ilya Loshchilov and Frank Hutter. Decoupled weight decay regularization. In *International Conference on Learning Representations*, 2017. 1

[29] Yongxi Lu, Abhishek Kumar, Shuangfei Zhai, Yu Cheng, Tara Javidi, and Rogério Schmidt Feris. Fully-adaptive feature sharing in multi-task networks with applications in person attribute classification. *2017 IEEE Conference on Computer Vision and Pattern Recognition (CVPR)*, pages 1131–1140, 2016. 2, 3

[30] Rabeeh Karimi Mahabadi, Sebastian Ruder, Mostafa Dehghani, and James Henderson. Parameter-efficient multi-task fine-tuning for transformers via shared hypernetworks. In *Proceedings of the 59th Annual Meeting of the Association for Computational Linguistics and the 11th International Joint Conference on Natural Language Processing (Volume 1: Long Papers)*, pages 565–576, 2021. 2, 3, 7

[31] Kevins-Koktsi Maninis, Ilija Radosavovic, and Iasonas Kokkinos. Attentive single-tasking of multiple tasks. In *Proceedings of the IEEE/CVF conference on computer vision and pattern recognition*, pages 1851–1860, 2019. 3

[32] Jonas Pfeiffer, Andreas Rücklé, Clifton Poth, Aishwarya Kamath, Ivan Vulic, Sebastian Ruder, Kyunghyun Cho, and Iryna Gurevych. Adapterhub: A framework for adapting transformers. *EMNLP 2020*, page 46, 2020. 3

[33] Jonas Pfeiffer, Aishwarya Kamath, Andreas Rücklé, Kyunghyun Cho, and Iryna Gurevych. Adapterfusion: Non-destructive task composition for transfer learning. In *Proceedings of the 16th Conference of the European Chapter of the Association for Computational Linguistics: Main Volume*, pages 487–503, 2021. 2

[34] Dmitry Senushkin, Nikolay Patakin, Arseny Kuznetsov, and Anton Konushin. Independent component alignment for multi-task learning. In *Proceedings of the IEEE/CVF Conference on Computer Vision and Pattern Recognition*, pages 20083–20093, 2023. 3

[35] Nathan Silberman, Derek Hoiem, Pushmeet Kohli, and Rob Fergus. Indoor segmentation and support inference from rgbd images. In *Computer Vision–ECCV 2012: 12th European Conference on Computer Vision, Florence, Italy, October 7–13, 2012, Proceedings, Part V 12*, pages 746–760. Springer, 2012. 5

[36] Yi-Lin Sung, Varun Nair, and Colin A Raffel. Training neural networks with fixed sparse masks. *Advances in Neural Information Processing Systems*, 34:24193–24205, 2021. 2, 3

[37] Gemini Team, Rohan Anil, Sebastian Borgeaud, Jean-Baptiste Alayrac, Jiahui Yu, Radu Soricut, Johan Schalkwyk, Andrew M Dai, Anja Hauth, Katie Millican, et al. Gemini: a family of highly capable multimodal models. *arXiv preprint arXiv:2312.11805*, 2023. 1

[38] Hugo Touvron, Louis Martin, Kevin Stone, Peter Albert, Amjad Almahairi, Yasmine Babaei, Nikolay Bashlykov, Soumya Batra, Prajjwal Bhargava, Shruti Bhosale, et al. Llama 2: Open foundation and fine-tuned chat models. *arXiv preprint arXiv:2307.09288*, 2023. 1

[39] Simon Vandenhende, Stamatios Georgoulis, Bert De Brabandere, and Luc Van Gool. Branched multi-task networks: Deciding what layers to share. *Proceedings BMVC 2020*, 2019. 2, 3

[40] Simon Vandenhende, Stamatios Georgoulis, and Luc Van Gool. Mti-net: Multi-scale task interaction networks for multi-task learning. In *Computer Vision–ECCV 2020: 16th European Conference, Glasgow, UK, August 23–28, 2020, Proceedings, Part IV 16*, pages 527–543. Springer, 2020. 5

[41] Simon Vandenhende, Stamatios Georgoulis, Wouter Van Gansbeke, Marc Proesmans, Dengxin Dai, and Luc Van Gool. Multi-task learning for dense prediction tasks: A survey. *IEEE transactions on pattern analysis and machine intelligence*, 44(7):3614–3633, 2021. 3, 5

[42] Jingdong Wang, Ke Sun, Tianheng Cheng, Borui Jiang, Chaorui Deng, Yang Zhao, Dong Liu, Yadong Mu, Mingkui Tan, Xinggang Wang, et al. Deep high-resolution representation learning for visual recognition. *IEEE Transactions on Pattern Analysis and Machine Intelligence*, 43(10):3349–3364, 2020. 6

[43] Yaqing Wang, Sahaj Agarwal, Subhabrata Mukherjee, Xiaodong Liu, Jing Gao, Ahmed Hassan, and Jianfeng Gao. Adamix: Mixture-of-adaptations for parameter-efficient model tuning. In *Proceedings of the 2022 Conference on Empirical Methods in Natural Language Processing*, pages 5744–5760, 2022. 2

[44] Yi Xin, Siqi Luo, Haodi Zhou, Junlong Du, Xiaohong Liu, Yue Fan, Qing Li, and Yuntao Du. Parameter-efficient fine-tuning for pre-trained vision models: A survey. *arXiv preprint arXiv:2402.02242*, 2024. 2

[45] Dan Xu, Wanli Ouyang, Xiaogang Wang, and Nicu Sebe. Pad-net: Multi-tasks guided prediction-and-distillation network for simultaneous depth estimation and scene parsing. In *Proceedings of the IEEE Conference on Computer Vision and Pattern Recognition*, pages 675–684, 2018. 5

[46] Hanrong Ye and Dan Xu. Inverted pyramid multi-task transformer for dense scene understanding. In *European Conference on Computer Vision*, pages 514–530. Springer, 2022. 5

[47] Jun Yu, Yutong Dai, Xiaokang Liu, Jin Huang, Yishan Shen, Ke Zhang, Rong Zhou, Eashan Adhikarla, Wenxuan Ye, Yixin Liu, et al. Unleashing the power of multi-task learning: A comprehensive survey spanning traditional, deep, and pretrained foundation model eras. *arXiv preprint arXiv:2404.18961*, 2024. 3

[48] Tianhe Yu, Saurabh Kumar, Abhishek Gupta, Sergey Levine, Karol Hausman, and Chelsea Finn. Gradient surgery for

multi-task learning. *Advances in Neural Information Processing Systems*, 33:5824–5836, 2020. [2](#)

[49] Elad Ben Zaken, Yoav Goldberg, and Shauli Ravfogel. Bitfit: Simple parameter-efficient fine-tuning for transformer-based masked language-models. In *Proceedings of the 60th Annual Meeting of the Association for Computational Linguistics (Volume 2: Short Papers)*, pages 1–9, 2022. [3](#)

[50] Qingru Zhang, Minshuo Chen, Alexander Bukharin, Pengcheng He, Yu Cheng, Weizhu Chen, and Tuo Zhao. Adaptive budget allocation for parameter-efficient fine-tuning. In *The Eleventh International Conference on Learning Representations*, 2023. [2](#), [3](#)

Parameter-Efficient Multi-Task Learning via Progressive Task-Specific Adaptation

Supplementary Material

7. Training Hyperparameters

PASCAL. We replicate the hyperparameters from Agiza et al. [3] for fine-tuning the models on the PASCAL dataset. Specifically, we use the AdamW optimizer [28] with a batch size of 32, a learning rate of 3.125×10^{-5} , and a weight decay of 0.05. The models are fine-tuned for 300 epochs, with evaluations every 20 epochs. We use a linear warmup for the first 20 epochs, followed by a cosine annealing learning rate scheduler. For the LoRA modules, a dropout rate of 0.05 and a scaling of 4 are used. We also apply the following data augmentations – `RandomHorizontalFlip`, `RandomScale` ranging from 0.75 to 1.25, and `RandomRotate` ranging from -20 to 20.

NYUD-v2. We use a batch size of 6 and a learning rate of 10^{-4} for NYUD-v2. All other hyperparameters remain the same as PASCAL. We also apply the following data augmentations – `RandomHorizontalFlip` and `RandomScale` with possible scales of 1, 1.2, and 1.5.

8. Additional Results

In this section, we present additional experiments on the PASCAL and NYUD-v2 datasets. Continuing from Section 4.5, Table 5 illustrates the performance of TGLoRA for varying trainable parameters. The rank of the low-rank modules in TGLoRA layers controls this number. The table also shows the performance of “Single Task – LoRA” and “MTL – LoRA” when the attention and MLP layers are augmented with TGLoRA and when the patch embedding, patch merging, layer normalization, and position bias layers are unfrozen during fine-tuning. Note that unfreezing additional layers results in more trainable parameters in the single-task models, as these layers are unfrozen in the individual models. Hence, the “ATTN + MLP + OTHERS” configuration has more trainable parameters than the corresponding TGLoRA or MTL – LoRA counterparts. Our experiments show that progressive task-specific adaptation performs better than individual single-task and shared multi-task adaptations when different layers are augmented with TGLoRA or when additional layers are unfrozen during fine-tuning.

9. Computational Budget vs Performance

The tree structure offers a trade-off between model performance and inference cost. For instance, using 6.89M

parameters for PASCAL-Context, and assigning one, one, two, and four task groups to the first through fourth stages, respectively, results in $\Delta m = +3.93\%$ with 38.37 GMacs. Similarly, configuring the stages with one, two, two, and four task groups results in $\Delta m = +4.21\%$ and 41.38 GMacs.

Table 5. Additional results on the PASCAL dataset. The number of trainable parameters is controlled by varying the rank of the LoRA modules. Δm is computed based on the single-task performance from Table 1. The experiments are repeated three times with different random seeds, and the average is reported.

Trainable Layers	SemSeg (mIoU \uparrow)	Human Parts (mIoU \uparrow)	Saliency (mIoU \uparrow)	Normals (rmse \downarrow)	Δm (% \uparrow)	Trainable Params (M \downarrow)
<i>TGLoRA</i>						
ATTN + MLP + OTHERS	70.66	60.48	65.56	16.65	+3.82	5.41
	70.66	59.76	65.15	16.79	+3.17	4.68
ATTN + MLP	70.40	60.01	65.34	16.90	+3.10	3.81
	70.34	59.17	64.84	17.13	+2.21	3.08
ATTN	70.33	58.90	64.72	17.45	+1.61	2.65
	70.27	58.37	64.09	17.69	+0.79	2.37
<i>MTL - LoRA</i>						
ATTN + MLP + OTHERS	67.62	59.22	65.28	16.86	+1.78	6.89
	68.07	59.07	64.96	17.11	+1.41	5.41
	68.52	58.78	64.29	17.30	+0.93	4.68
ATTN + MLP	68.02	58.78	64.77	17.33	+0.89	3.81
	68.35	58.30	63.99	17.62	+0.10	3.08
ATTN	68.25	58.42	64.38	17.57	+0.34	3.20
	68.52	58.11	63.73	17.92	-0.43	2.65
	68.62	57.65	63.23	18.20	-1.17	2.37
<i>Single Task - LoRA</i>						
ATTN + MLP + OTHERS	71.16	59.42	66.21	16.41	4.17	11.69
	71.32	59.05	65.78	16.58	3.68	10.21
	71.37	58.70	65.35	16.67	3.25	9.48
ATTN + MLP	70.83	58.15	65.54	16.95	2.52	3.81
	70.82	57.70	64.97	17.14	1.84	3.08
ATTN	70.65	57.78	65.2	17.25	1.75	3.20
	70.63	57.47	64.75	17.48	1.12	2.65
	70.52	56.99	64.11	17.74	0.26	2.37

Table 6. Additional results on the NYUD-v2 dataset. Δm is computed based on the single-task performance from Table 2. The experiments are repeated three times with different random seeds, and the averages are reported.

Trainable Layers	SemSeg (mIoU \uparrow)	Normals (rmse \downarrow)	Depth (rmse \downarrow)	Δm (% \uparrow)	Trainable Params (M \downarrow)
<i>MTL - LoRA</i>					
ATTN + MLP + OTHERS	41.03	25.01	0.6216	-1.48	7.53
	41.92	25.81	0.6309	-2.37	3.15
<i>Single Task - LoRA</i>					
ATTN + MLP + OTHERS	42.10	24.49	0.6310	-0.40	10.73
	41.69	25.34	0.6376	-2.26	3.15